

See discussions, stats, and author profiles for this publication at: <https://www.researchgate.net/publication/232366083>

Large deflection of cantilever beams with geometric non-linearity: Analytical and numerical approaches

Article in International Journal of Non-Linear Mechanics · June 2008

DOI: 10.1016/j.ijnonlinmec.2007.12.020

CITATIONS
137

READS
1,709

3 authors:



Atanu Banerjee
Indian Institute of Technology Guwahati

15 PUBLICATIONS 252 CITATIONS

[SEE PROFILE](#)



Bishakh Bhattacharya
Indian Institute of Technology Kanpur

146 PUBLICATIONS 685 CITATIONS

[SEE PROFILE](#)



A. K. Mallik
Indian Institute of Engineering Science and Technology, Shibpur
97 PUBLICATIONS 2,167 CITATIONS

[SEE PROFILE](#)

Some of the authors of this publication are also working on these related projects:



SPARC Project on Metasandwich [View project](#)



Torus and Viscoelastic Modeling [View project](#)



ARTICLE IN PRESS

Available online at www.sciencedirect.com



International Journal of Non-Linear Mechanics III (III) III-III

INTERNATIONAL JOURNAL OF

**NON-LINEAR
MECHANICS**

www.elsevier.com/locate/nlm

1

3

Large deflection of cantilever beams with geometric non-linearity: Analytical and numerical approaches

A. Banerjee*, B. Bhattacharya, A.K. Mallik

5

Department of Mechanical Engineering, Indian Institute of Technology, Kanpur, UP 208016, India

Received 7 May 2007; received in revised form 22 December 2007; accepted 22 December 2007

7 Abstract

9

Non-linear shooting and Adomian decomposition methods have been proposed to determine the large deflection of a cantilever beam under arbitrary loading conditions. Results obtained only due to end loading are validated using elliptic integral solutions. The non-linear shooting method gives accurate numerical results while the Adomian decomposition method yields polynomial expressions for the beam configuration. With high load parameters, occurrence of multiple solutions is discussed with reference to possible buckling of the beam-column. An example of concentrated intermediate loading (cantilever beam subjected to two concentrated self-balanced moments), for which no closed form solution can be obtained, is solved using these two methods. Some of the limitations and recipes to obviate these are included. The methods will be useful toward the design of compliant mechanisms driven by smart actuators.

15

© 2008 Published by Elsevier Ltd.

Keywords: Large deflection beams; Compliant mechanism; Non-linear shooting; Adomian-polynomials

17

1. Introduction

19

The structural deformation of a single piece flexible member is utilized to generate a desired output movement in what is commonly known as a compliant mechanism. In such a mechanism, one or more segments is/are subjected to various types of external loadings, which include actuation forces/moment and reactions from the surroundings. In the literature on compliant mechanisms, each segment is modeled as a cantilever beam. Due to large deflection, the bending displacements are obtained from the Euler-Bernoulli beam theory taking into account the geometric non-linearity. Solution to the resulting non-linear differential equation has been obtained in terms of elliptic integrals of the first and second kind [1]. Such analytical solutions are possible only for simple geometry (uniform cross-section) and loading conditions like forces at the free end. Howell and Midha [2] have used this approach for developing a pseudo-rigid body model of a compliant cantilever subjected to end forces only. Numerical schemes have also been

proposed [3] where the forces along with moments are applied only at the free end. The occurrence of any inflection point within the beam segment requires special attention. More recently, Kimball and Tsai [4] have solved the large deflection problem under combined end loadings using elliptic integrals and differential geometry. In this method there is no need to locate the inflection point, if any, within the beam. However, for intermediate loading and beams with varying geometry, obtaining solution using elliptic integral solutions require complex algorithm with iterative procedure.

For a smart compliant mechanism, i.e., a compliant mechanism actuated by smart materials based actuators, besides external forces working at the free end of the cantilever beam (typifying the model of a compliant segment), actuators may apply forces and moments at some intermediate locations. In this paper, two simple methods, one numerical method called non-linear shooting [5] and another semi-analytical method known as Adomian decomposition [6] have been proposed to obtain large deflection of a cantilever beam including geometric non-linearity. Both these methods are capable of handling loading at intermediate locations besides end forces and moments. First, the solution procedure is discussed for end loading and

37
39
41
43
45
47
49
51
53
55
57
59

* Corresponding author.

E-mail address: atanub@iitk.ac.in (A. Banerjee).

the results are compared with those obtained by using elliptic integrals [2]. The convergence of the Adomian decomposition method, while treating large deflection of an Euler–Bernoulli beam, is also discussed. Secondly, the equilibrium equation of a cantilever beam actuated through self-balanced moments has been derived and solved using these two methods. The self-balanced moment acting within the continuum can be interpreted as the effect of a piezo patch [7–10] attached to the beam.

2. Formulation of large deflection beam problem

Fig. 1 shows a cantilever beam in deformed configuration under a non-following end force F and an end moment M_0 [2–4], which can be decomposed into horizontal (P) and vertical (nP) components. The moment acting at any point (x, y) on the beam can be written as

$$M_{(x,y)} = P(a - x) + nP(b - y) + M_0, \quad (1)$$

where (a, b) is the location of the deflected end point of the beam. Using the Euler–Bernoulli moment–curvature relationship

$$EI \frac{d\theta}{ds} = P(a - x) + nP(b - y) + M_0, \quad (2)$$

where EI is the flexural rigidity of the beam, assumed to be constant throughout the length of the beam; θ is the slope at any point (x, y) and s is the distance of that point along the length of the beam from its fixed end. Total length of the undeformed beam L is assumed to remain same after deformation. Differentiating Eq. (2) and substituting

$$\frac{dx}{ds} = \cos \theta \quad \text{and} \quad \frac{dy}{ds} = \sin \theta$$

we get

$$\frac{d^2\theta}{ds^2} = -\frac{P}{EI}(\cos \theta + n \sin \theta). \quad (3)$$

Eq. (3) involves cosine and sine terms of the dependent variable, hence it is a non-linear differential equation. To solve this second order differential equation we need two boundary conditions, which are $(\theta|_{s=0} = 0)$ and $(\frac{d\theta}{ds}|_{s=L} = \frac{M_0}{EI})$.

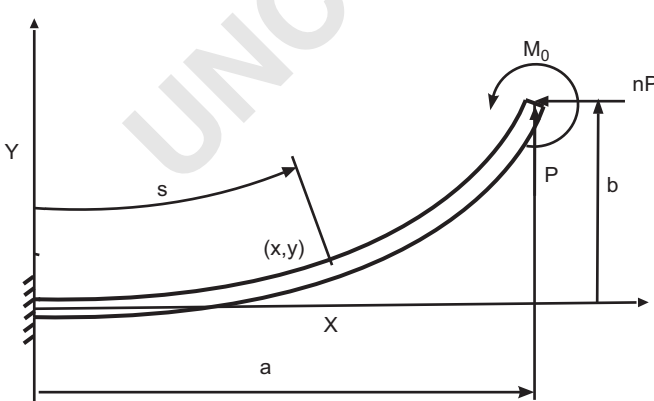


Fig. 1. Cantilever beam subjected to non-following force ' F '.

2.1. Problem definition

$$\left. \begin{array}{l} \text{D.E.} \quad \frac{d^2\theta}{ds^2} = -\frac{P}{EI}(\cos \theta + n \sin \theta) \\ \text{B.C.} \quad \left. \begin{array}{l} \theta|_{s=0} = 0 \\ \frac{d\theta}{ds} \Big|_{s=L} = \beta \end{array} \right. \end{array} \right\}, \quad (4)$$

where $\beta = 0$ if there is no moment acting at the free end.

2.2. Existing solutions for end loading

In this section previous analytical and numerical approaches [2–4] are briefly discussed. Eq. (3) can be written as

$$\begin{aligned} \frac{d}{d\theta} \left[\frac{d\theta}{ds} \right] \frac{d\theta}{ds} &= -\frac{P}{EI}(\cos \theta + n \sin \theta) \Rightarrow \frac{d}{d\theta} \left[\frac{1}{2} \left(\frac{d\theta}{ds} \right)^2 \right] \\ &= -\frac{P}{EI}(\cos \theta + n \sin \theta). \end{aligned} \quad (5)$$

Integrating with respect to θ and using the moment boundary condition at $s = L$, i.e., $EI \frac{d\theta}{ds} = M_0$ one obtains,

$$\left(\frac{d\theta}{ds} \right)^2 = \frac{2P}{EI}(\lambda - \sin \theta + n \cos \theta), \quad (6)$$

where $\lambda = \sin \theta_0 - n \cos \theta_0 + \kappa_0$, $\kappa_0 = \frac{M_0^2}{2PEI}$ and θ_0 is the end slope of the beam. Eq. (6) can be written as

$$\begin{aligned} \sqrt{\frac{2P}{EI}} \int_0^L ds &= \int_0^{\theta_0} \sqrt{(\lambda - \sin \theta + n \cos \theta)} d\theta \Rightarrow \alpha_0 \\ &= \frac{1}{\sqrt{2}} \int_0^{\theta_0} \sqrt{(\lambda - \sin \theta + n \cos \theta)} d\theta, \end{aligned} \quad (7)$$

where $\alpha_0 = \sqrt{\frac{PL^2}{EI}}$. Further modification of Eq. (6) yields

$$\begin{aligned} \frac{d\theta}{dx} \frac{dx}{ds} &= \sqrt{\frac{2P}{EI}(\lambda - \sin \theta + n \cos \theta)} \Rightarrow \int_0^a \frac{dx}{L} \\ &= \frac{1}{\sqrt{2}\alpha_0} \int_0^{\theta_0} \frac{\cos \theta d\theta}{\sqrt{(\lambda - \sin \theta + n \cos \theta)}} \end{aligned} \quad (8)$$

and

$$\begin{aligned} \frac{d\theta}{dy} \frac{dy}{ds} &= \sqrt{\frac{2P}{EI}(\lambda - \sin \theta + n \cos \theta)} \Rightarrow \int_0^b \frac{dy}{L} \\ &= \frac{1}{\sqrt{2}\alpha_0} \int_0^{\theta_0} \frac{\sin \theta d\theta}{\sqrt{(\lambda - \sin \theta + n \cos \theta)}}. \end{aligned} \quad (9)$$

Eqs. (7)–(9) are solved in order to obtain the end point coordinates of the deformed beam under combined end loadings. Howell and Midha [2] solved these equations using Jacobian elliptic integrals of first and second types by considering only an end force. Saxena and Kramer [3] proposed a numerical integration scheme for combined end loading. However, the occurrence of any inflection point within the beam requires special consideration. The method proposed by Kimball and Tsai [4] does not need to locate the inflection point. The solutions

1 are found from Ref. [4, Eqs. (46)–(55)]. However, two different
2 sets of equations are required to be used depending on the
3 presence or absence of an inflection point.

4 The use of elliptic integral solutions is straight forward if the
5 end slope is provided. The end deflection can then be obtained
6 from Ref. [4, Eqs. (46)–(55)]. Furthermore, in presence of load-
7 ings within the beam (besides end loading) one needs to split
8 the beam into several cantilevers each having only end loads.
9 Consequently, a complicated iterative algorithm is needed to
solve such a problem.

10 In sections to follow, it is shown that the proposed non-
11 linear shooting method can take into account any type of inter-
12 mediate loading (static, concentrated or discretely distributed)
13 in a straight forward and simple manner. The proposed semi-
14 analytical Adomian decomposition method involves initial
15 algebraic computation, which can be easily done by Matlab or
16 Maple. But once the expression for $\theta(s)$ is obtained, the rest of
17 the procedure is simple. These two methods, capable of han-
18 dling complicated geometry and loading, are discussed below.

3. Non-linear shooting method

21 In the non-linear shooting method the boundary value prob-
22 lem (BVP) is converted into an initial value problem (IVP)
23 with an assumed curvature at the fixed end, i.e., $\frac{d\theta}{ds}|_{s=0}$. Using
24 the initial conditions the differential equation is solved using
25 Runge–Kutta method and the assumed initial condition is mod-
26 ified till the second boundary condition is satisfied. The method
27 of non-linear shooting including the proof is available in [5].
28 But the problem under investigation requires slight modification
29 of the approach given in [5]. This modification is explained
below.

30 Here IVP is posed as

$$\left. \begin{array}{l} \text{D.E. } \frac{d^2\theta}{ds^2} = -\frac{P}{EI}(\cos \theta + n \sin \theta) \\ \text{I.C. } \left\{ \begin{array}{l} \theta|_{s=0} = 0 \\ \frac{d\theta}{ds}\Big|_{s=0} = m_k \end{array} \right. \end{array} \right\}, \quad (10)$$

31 where m_k is assumed to be the first derivative of the slope at the
32 fixed end at the k th iteration step. Thus, the error involved can
33 be determined as $\text{error} = [\left(\frac{d\theta}{ds}\right)|_{s=L} - \beta]$ which is to be made less
34 than a prescribed value, by properly guiding m_k . In this paper,
35 Newton–Raphson method has been followed. Now m_k in the
36 k th step can be calculated from that of the $(k-1)$ th step using

$$m_k = m_{k-1} - \frac{\text{(error)}}{\frac{\partial}{\partial m} \left(\frac{d\theta}{ds} \Big|_{s=L} \right)}. \quad (11)$$

37 The difference between this problem and that used to explain
38 the shooting method in [5] is, instead of having $\theta|_{s=L}$ as the
39 second B.C., we have its derivative specified. Thus, $\frac{\partial}{\partial m} (\frac{d\theta}{ds}|_{s=L})$
40 is to be calculated instead of $\frac{\partial}{\partial m}[\theta|_{s=L}]$. The term $\frac{\partial}{\partial m} (\frac{d\theta}{ds}|_{s=L})$
41 can be determined as follows.

42 Eq. (10) can be written as

$$\theta'' = f(s, \theta, \theta'). \quad (12)$$

Differentiating Eq. (12) with respect to m we get

$$\frac{\partial \theta''}{\partial m} = f_{,s} \frac{\partial s}{\partial m} + f_{,\theta} \frac{\partial \theta}{\partial m} + f_{,\theta'} \frac{\partial \theta'}{\partial m}. \quad (13)$$

Since s and m are independent, Eq. (13) becomes

$$\frac{\partial \theta''}{\partial m} = f_{,\theta} \frac{\partial \theta}{\partial m} + f_{,\theta'} \frac{\partial \theta'}{\partial m}. \quad (14)$$

This can be written as

$$\psi'' = f_{,\theta}\psi + f_{,\theta'}\psi', \quad (15)$$

where $\psi = \frac{\partial \theta}{\partial m}$, which yields $\psi|_{s=0} = 0$ and $\psi'|_{s=0} = \frac{\partial}{\partial m}(\frac{d\theta}{ds}|_{s=0}) = 1$.

All these result in another IVP defined as

$$\left. \begin{array}{l} \text{D.E. } \psi'' = f_{,\theta}\psi + f_{,\theta'}\psi' \\ \text{I.C. } \left\{ \begin{array}{l} \psi|_{s=0} = 0 \\ \psi'|_{s=0} = 1 \end{array} \right. \end{array} \right\}. \quad (16)$$

Solving Eq. (16) one gets $\frac{\partial}{\partial m}(\frac{d\theta}{ds}|_{s=L})$, which is nothing but $\psi'|_{s=L}$.

Eqs. (10) and (16) are solved simultaneously using fourth order Runge–Kutta method. The normalized load parameter $\alpha = \frac{PL^2}{EI}$ is used for obtaining numerical results. For given α and N , $\frac{P}{EI}$ can be computed and is used to solve Eq. (10).

In presence of an end moment, one has to change β to non-zero, i.e., $\beta = \frac{M_0}{EI}$, where M_0 is the moment applied at the end of the beam. Now β is expressed in terms of the normalized moment parameter $\kappa = M_0 L/EI$. Versatility of this method allows handling of the cantilever configuration with and without inflection point (for negative and positive end moments, respectively) in the same fashion.

4. Adomian decomposition method

Numerous BVP have been solved using Adomian decomposition method [11,12]. Here the decomposition method is discussed in a nutshell. Let us consider a non-linear differential equation in the form:

$$\Lambda u + \Pi u + Nu = g, \quad (17)$$

where Λ is an invertible linear operator, Π is the remaining linear part and N is the non-linear operator. The general solution is decomposed into $u = \sum_{n=0}^{\infty} u_n$, where u_0 is the complete solution of $\Lambda u = g$. Eq. (17) can be written as

$$\Lambda u = g - \Pi u - Nu. \quad (18)$$

Since Λ is an invertible linear operator, Eq. (18) is expressed as

$$u = \Lambda^{-1}g - \Lambda^{-1}\Pi u - \Lambda^{-1}Nu. \quad (19)$$

If $\Lambda \equiv \frac{d^n}{dt^n}$ with t as an independent variable then Λ^{-1} is the n -fold definite integral with respect to t with limits from 0 to t . Thus, if we have a second order linear operator, Eq. (19) yields

$$u = u(0) + u'(0)t + \Lambda^{-1}g - \Lambda^{-1}\Pi u - \Lambda^{-1}Nu, \quad (20)$$

which can be written as

$$u = a + bt + \Lambda^{-1}g - \Lambda^{-1}\Pi u - \Lambda^{-1}Nu. \quad (21)$$

For an IVP $a = u(0)$ and $b = u'(0)$ are specified. On the other hand for a BVP $a = u(0)$ is specified but $b = u'(0)$ is to be determined by satisfying the second boundary condition of $u(t)$. Now $u_0 = a + bt + \Lambda^{-1}g$ and the solution is obtained as

$$u = \sum_{n=0}^{\infty} u_n. \quad (22)$$

In Eq. (20) Nu can be written as $Nu = \sum_{n=0}^{\infty} A_n(u_0, u_1, u_2, u_3, \dots, u_n)$, where A_n 's elements of a special set of polynomials determined from the particular non-linear term $Nu = f(u)$, called Adomian polynomials [6]. A_n 's are calculated as [13,14]

$$\left. \begin{aligned} A_0 &= f(u_0) \\ A_1 &= u_1 \frac{d}{du_0} [f(u_0)] \\ A_2 &= u_2 \frac{df(u_0)}{du_0} + (u_1^2/2!) \frac{d^2 f(u_0)}{du_0^2} \\ A_3 &= u_3 \frac{df(u_0)}{du_0} + (u_1 u_2) \frac{d^2 f(u_0)}{du_0^2} + (u_1^3/3!) \frac{d^3 f(u_0)}{du_0^3} \\ \dots \end{aligned} \right\}. \quad (23)$$

Thus, the general solution becomes

$$u = u_0 - \Lambda^{-1}\Pi \sum_{n=0}^{\infty} u_n - \Lambda^{-1} \sum_{n=0}^{\infty} A_n, \quad (24)$$

where $u_0 = \eta + L^{-1}g$ such that $L\eta = 0$.

Finally u_{n+1} can be written as [13]

$$u_{n+1} = -\Lambda^{-1}\Pi u_n - \Lambda^{-1}A_n. \quad (25)$$

Using Eq. (25) and known u_0 , one can calculate u_1, u_2, \dots, u_n and the solution is obtained from Eq. (22). The proof of convergence is given in [15–18]. Two different approaches of using this method for the problem under investigation follow.

4.1. Solving beam problem using Adomian decomposition

4.1.1. Procedure I

Integrating Eq. (10) twice with respect to s

$$\theta(s) = \theta(0) + \left. \frac{d\theta}{ds} \right|_{s=L} s + \int_0^s \int_L^t N(\theta) ds dt, \quad (26)$$

where $N(\theta) = -\frac{P}{EI}(\cos \theta + n \sin \theta)$. Applying the B.C.'s described in Eq. (4), Eq. (26) yields

$$\theta(s) = \beta s + \int_0^s \int_L^t N(\theta) ds dt, \quad (27)$$

Taking, $\theta_0 = 0$ all other θ_n 's are calculated using Eqs. (23), (25) and (27). Thus, the solution can be written as $\theta(s) = \sum_{n=1}^m \theta_n$, where $(m+1)$ th term onwards will have insignificant contribution. Once $\theta(s)$ is known, the coordinates of any point on the beam $(x(s), y(s))$ can be obtained by using $\frac{dx}{ds} = \cos \theta$ and $\frac{dy}{ds} = \sin \theta$.

4.1.2. Procedure II

Integrating Eq. (10) twice with respect to s one gets

$$\theta(s) = \theta(0) + \left. \frac{d\theta}{ds} \right|_{s=0} s + \int_0^s \int_0^t N(\theta) ds dt. \quad (28)$$

Assuming $c = \left. \frac{d\theta}{ds} \right|_{s=0}$ and following procedure I, $\theta(s)$ is obtained, from which c is determined satisfying the B.C.

$$\left. \frac{d\theta}{ds} \right|_{s=L} = \beta.$$

Though both the procedures satisfy the same D.E. and the same set of B.C.'s, the second one is more effective for large values of load parameters as will be discussed later.

The expressions for $\theta(s)$ as a function of c, α, n and κ are computed considering up to the 8th term of the Adomian polynomials and the details are given in Appendix A.

5. Cantilever beam under self-balanced moment and external load

The effect of a pair of piezo patches, mounted on two opposite sides of a cantilever beam driven out of phase is modeled [7–10] as two concentrated self-balanced moment acting at the edge of the piezo patches. The magnitude of the moments depends on the applied voltage across the piezo and its material properties. In this section, a large deflection cantilever beam has been modeled under self-balanced moments as well as external forces at the free end and solved using the above discussed methods.

5.1. Non-linear shooting method

Fig. 2 shows the deformed configuration of a cantilever beam subjected to two equal and opposite moments applied at intermediate locations together with a force applied at the free end. The moments are acting at distances l_1 and l_2 from the fixed end. Thus, the bending moment at a point (x, y) is given by

$$M_{(x,y)} = P(a-x) + nP(b-y) + M_1[u(s-l_1) - u(s-l_2)], \quad (29)$$

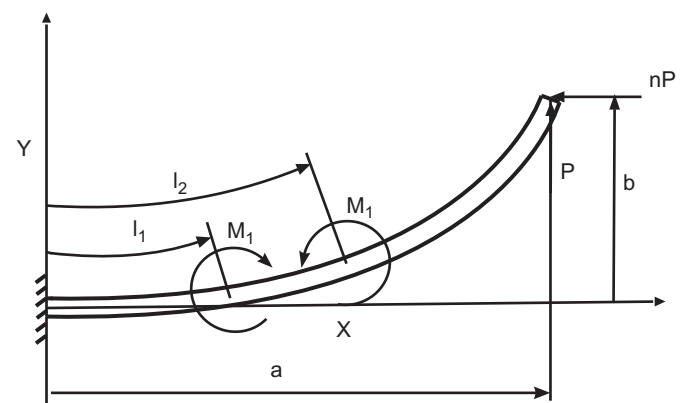


Fig. 2. Cantilever beam subjected to self-balanced moment and end loads.

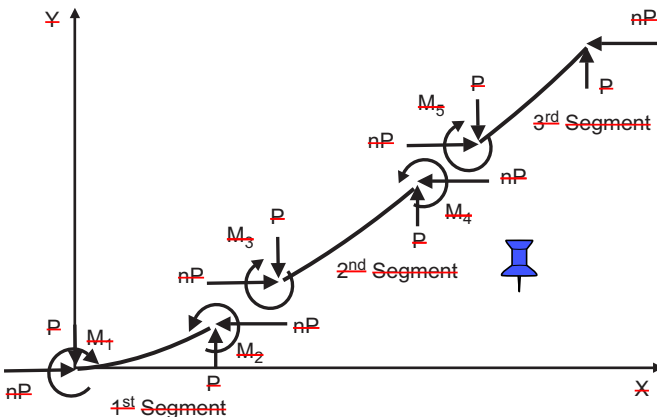


Fig. 3. Free body diagram of the three segments of the cantilever beam.

1 where $u(s)$ is the unit step function defined as $u(s) = 0$ for
2 $s < 0$ and $u(s) = 1$ for $s \geq 0$.

3 The Euler–Bernoulli beam theory yields

$$EI \frac{d\theta}{ds} = P(a - x) + nP(b - y) \\ + M_1[u(s - l_1) - u(s - l_2)]. \quad (30)$$

5 Differentiating Eq. (30) with respect to s one gets

$$\frac{d^2\theta}{ds^2} = -\frac{P}{EI}(\cos \theta + n \sin \theta) + M_1[\delta(s - l_1) - \delta(s - l_2)], \quad (31)$$

7 where $\delta(s)$ is the Dirac-Delta function defined as $\delta(s) = 0$ if
9 $s \neq 0$ and $\delta(s) \rightarrow \infty$ if $s = 0$. Here, $\delta(s)$ can be replaced by a
11 sharply rising continuous function such that $\int_{-\infty}^{\infty} \delta(s) ds = 1$ is
13 satisfied. The rest of the procedure is same as discussed earlier
15 in Section 3. First the curvature at the fixed end of the cantilever,
i.e., $\frac{d\theta}{ds}|_{s=0} = c$ is assumed for solving Eq. (31) using fourth order
Runge–Kutta method and c is varied using Newton–Raphson
method such that the moment boundary condition specified at
the free end is satisfied. The actuating moment M_1 is normalized
as $\tau = \frac{M_1 L}{EI}$.

17 5.2. Adomian decomposition method

19 While using the Adomian decomposition method, first the
cantilever beam is discretized into three segments as shown in
Fig. 3, so that the self-balanced moments are acting just on
21 the end points of the intermediate section. Thus, the length of
the intermediate segment is same as that of the piezo actuator,
23 i.e., $(l_2 - l_1)$ and the first and last segments are of length l_1
25 and $(L - l_2)$, where L is the length of the entire beam. The
27 external forces in each of the segments are clearly depicted in
29 Fig. 3. Each of the segments is considered as a beam undergoing
large deformation for which the governing equation is solved
using Adomian decomposition method. Force and moment
equilibrium and the continuity of displacement and slope
are maintained at every junction.

5.2.1. 1st segment

Considering the first segment as a cantilever beam shown in
Fig. 3, the governing equation is obtained from Eq. (28) as

$$\theta_1(s_1) = \theta_1(0) + \left. \frac{d\theta_1}{ds_1} \right|_{s_1=0} s_1 \\ + K \int_0^s \int_0^t (\cos \theta_1 + n \sin \theta_1) ds_1 dt, \quad (32)$$

where $K = (-\frac{P}{EI})$ and $\theta_1(s_1)$ is the slope at any point of the first
segment at a distance s_1 from the fixed end along the length of
the beam. The B.C.'s are

$$\theta_1|_{s_1=0} = 0 \quad \text{and} \quad \left. \frac{d\theta_1}{ds_1} \right|_{s_1=0} = c,$$

where c is the unknown to be determined. The non-linear terms
of Eq. (32) can be expressed in terms of Adomian polynomials
and the solution $\theta_1(s_1)$ can be determined as a polynomial of s
and c using the decomposition method as illustrated in Section
4.1.

5.2.2. 2nd segment

The governing equation for the second segment is obtained
from Eq. (28) as

$$\theta_2(s_2) = \theta_2(0) + \left. \frac{d\theta_2}{ds_2} \right|_{s_2=0} s_2 \\ + K \int_0^s \int_0^t (\cos \theta_2 + n \sin \theta_2) ds_2 dt, \quad (33)$$

where $\theta_2(s_2)$ is the slope at any point on the second segment at
a distance s_2 from the left end of this particular segment along
its length. The B.C.'s are

$$\theta_2(0) = \theta_1(l_1) \quad \text{and} \quad \left. \frac{d\theta_2}{ds_2} \right|_{s_2=0} = \frac{M_3}{EI} = \left. \frac{d\theta_1}{ds_1} \right|_{s_1=l_1} + \frac{M_1}{EI},$$

where l_1 is the length of the first segment and M_1 is the actuating
moment. Solving Eq. (33) using Adomian decomposition
method, $\theta_2(s_2)$ can be computed as a polynomial of s_1 , s_2 , c
and M_1 .

5.2.3. 3rd segment

Similarly the governing equation for the third segment can
be written as

$$\theta_3(s_3) = \theta_3(0) + \left. \frac{d\theta_3}{ds_3} \right|_{s_3=0} s_3 \\ + K \int_0^s \int_0^t (\cos \theta_3 + n \sin \theta_3) ds_3 dt, \quad (34)$$

where $\theta_3(s_3)$ is the slope at any point on the third segment
which is at a distance s_3 from the left end of this particular
segment along its length. The B.C.'s can be written as

$$\theta_3(0) = \theta_2(l_2 - l_1) \quad \text{and}$$

$$\left. \frac{d\theta_3}{ds_3} \right|_{s_3=0} = \frac{M_5}{EI} = \left. \frac{d\theta_2}{ds_2} \right|_{s_2=(l_2-l_1)} - \frac{M_1}{EI},$$

1 where $(l_2 - l_1)$ is the length of the second segment. Following
 3 Adomian decomposition method $\theta_3(s)$ can be determined as a
 polynomial of s_1, s_2, s_3, c and M_1 .

5 Thus, $\theta(s)$, the slope at any point on the entire beam is known
 7 in terms of c and M_1 . Now c should be such that the moment
 9 at the end of the beam must be equal to that specified at the
 free end. Using this B.C., c is determined and thus $\theta(s)$ can
 be calculated at any point of the beam as a function of M_1 ,
 i.e., the actuating self-balancing moments. Once $\theta(s)$ is known,
 $(x(s), y(s))$ is obtained using $\frac{dx}{ds} = \cos \theta$ and $\frac{dy}{ds} = \sin \theta$.

11 6. Results and discussion

13 The results of non-linear shooting and Adomian decomposi-
 15 tion methods have been compared with the elliptic integral sol-
 17ution for the end loading conditions. First the end slope of the
 beam is computed from the non-linear shooting method for a
 given loading condition and then the same is used in the elliptic
 integral solutions to solve for the loading parameter (α_0 in Eq.
 19 (7) which is same as $\sqrt{\alpha}$) and the end coordinates of the beam.

21 Fig. 4a shows the deformed configuration of the cantilever
 23 beam due to the combined (force and moment) end loading
 25 computed using non-linear shooting and elliptic integral sol-
 27utions. Two cases are considered for comparison—Case A
 29 ($\alpha=0.1, \kappa=0.1$) and Case B ($\alpha=0.5, \kappa=-0.3$). The direction
 31 of forces and moment as shown in Fig. 1 are assumed to be
 33 positive. Each point (X, Y) on the beam is normalized as $(\frac{X}{L},$
 $\frac{Y}{L})$, where L is the length of the unstretched beam. For Case A
 35 in Fig. 4a, the moment within the beam is positive throughout,
 hence the slope of the beam increases monotonically, whereas
 for Case B, the end moment is opposing the moment due to end
 forces resulting in an inflection point (a point where moment is
 zero) within the beam. Both of the cases have been dealt with
 the same algorithm of the non-linear shooting method. No sepa-
 rate consideration depending on the absence or presence of
 any inflection point, as required while using the elliptic integral
 solution, is necessary.

37 In order to show the accuracy of the non-linear shooting
 39 solution, the results obtained by this method and that of the
 41 analytical solution (elliptic integral solution) are furnished in
 Table 1. The numerical results are obtained with a tolerance
 level for the error in the curvature as 10^{-5} . These are seen to
 be accurate up to three decimal places and further accuracy can
 be achieved by decreasing the allowable tolerance.

43 It is well established [19] that to ensure a unique solution to
 45 a BVP, the parameters involved must satisfy certain conditions.
 For the problem under consideration, unique solution is ‘guar-
 47anteed’, as shown in Appendix B, if the following condition is
 satisfied:

$$\alpha\sqrt{1+n^2} \leq \frac{\pi^2}{4}. \quad (35)$$

49 It may be mentioned that unique solution ‘may exist’ even if
 51 the above condition is violated. When multiple solutions exist,
 one of the possible solutions is yielded by the non-linear shoot-
 ing method depending on the initial estimate of $c = \frac{dx}{ds}|_{s=0}$.

To test the occurrence of multiple solutions, the initial es-
 53 timate of c was varied in the range $(-10 < c < 10)$ for differ-
 ent loading parameters. A case of a multiple solutions is illus-
 55 trated in Fig. 4b with condition (35) violated by a wide margin.
 It should be mentioned that both the deformed configurations
 57 shown in Fig. 4b can be kept in equilibrium under the given
 59 loading. It was seen that the first solution of Fig. 4b can be ob-
 61 tained if the loading is increased in small steps starting from a
 63 value satisfying condition (35). Further, it is necessary that the
 initial estimate of c at each successive loading step is provided
 by the final value of c obtained in the earlier step.

It is well known that the Euler buckling load (in absence
 65 of any transverse component) of a cantilever column is given
 by $\frac{\pi^2 EI}{4L^2}$. It is conjectured that multiple solutions are resulted
 67 due to buckling of this cantilever beam-column. Buckling is
 69 caused by the horizontal compressive load nP . The magnitude
 71 of the compressive load required to cause buckling depends on
 the transverse component as well. Non-linear shooting method
 converges to one of the buckled configurations depending on
 the initial estimate of c .

The direction and magnitude of the end load are specified
 75 by two parameters, viz., n and α . A larger value of n signifies
 77 a smaller ratio of the transverse to the axial load and vice
 versa. The sufficiency condition (35) indicates that uniqueness
 79 is guaranteed so long the resultant end load is less than the
 Euler buckling load. Obviously, this results in a conservative
 estimate of α to ensure uniqueness when n is finite.

Numerical simulations were carried out for various combi-
 81 nations of $n\alpha$ and n required to produce unique solution. The
 83 region below the curve A in Fig. 4c corresponds to necessary
 85 conditions on the load parameters to achieve unique solution.
 Condition (35) with equality sign is also shown by curve B in
 87 Fig. 4c. It may be seen that with $n=1$ condition (35) is violated
 for $\alpha > \frac{\pi^2}{4\sqrt{2}} \approx 1.745$. However, curve A in Fig. 4c suggests
 89 occurrence of unique solution with $\alpha < 4.24$. As $n \rightarrow \infty$, the
 91 entire end load becomes compressive and the sufficiency con-
 93 dition (35) tends to ‘necessary’ condition for uniqueness of the
 95 solution. The corresponding value of the horizontal load con-
 97sequently reaches the Euler buckling limit. On the other hand,
 99 for smaller values of n , the sufficiency condition (35) becomes
 101 too conservative for the estimate of α ensuring unique solution.

Figs. 5a and b show the deformed beam shape, obtained fol-
 103 lowing procedures I and II, respectively, of Adomian decom-
 105 position method. The results are compared with that obtained us-
 107 ing elliptic integral solutions. Only the effect of end forces has
 109 been considered here. From Fig. 5a it can be readily seen that,
 for low values of the load parameter (i.e., say up to $\alpha < 1.4$), the
 results match pretty well. However, for $\alpha \geq 1.4$ the difference
 starts to become significant and higher the value of α , larger
 is the deviation. In order to minimize this discrepancy, more
 number of terms is to be incorporated in the Adomian polynomi-
 als while approximating the non-linear terms of Eq. (4). This
 obviously increases the computational cost. Fig. 5a is obtained
 using up to the 8th term of the Adomian polynomials. Using
 procedure II and the same number of terms in Adomian polynomi-
 als, the deflected beam shape shows very little discrepancy

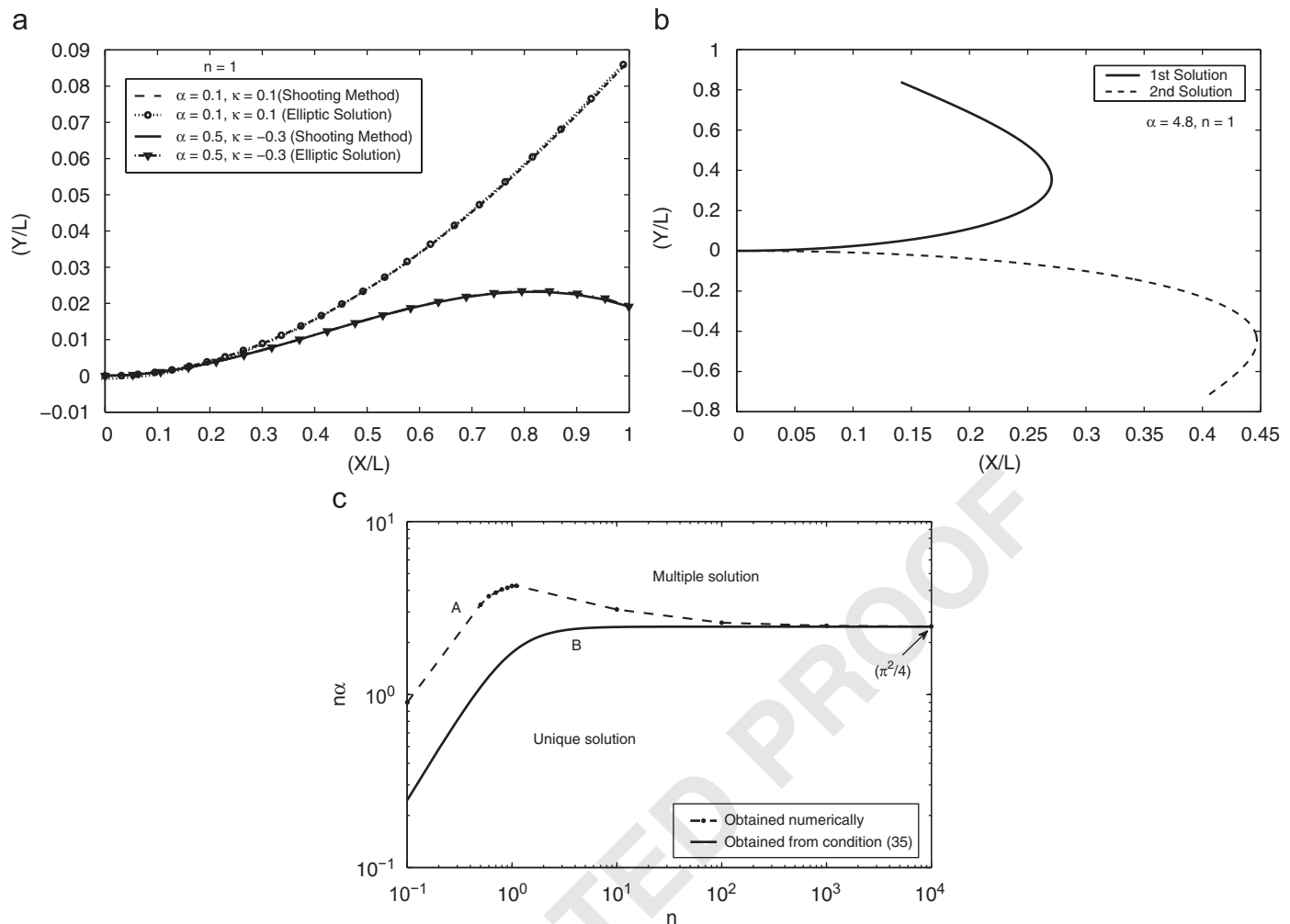


Fig. 4. (a) Deformed beam shape due to combined end loading; (b) multiple beam configuration obtained using non-linear shooting method; (c) sufficient and numerically computed necessary conditions for uniqueness.

Table 1
Comparison of numerical accuracy of the solutions obtained from elliptic integral, non-linear shooting and Adomian decomposition method

Loads	At $\bar{s} = 1$ elliptic solution		At $\bar{s} = 1$ shooting method		At $\bar{s} = 1$ Adomian method (up to 8th order terms)	
	\bar{x}	\bar{y}	\bar{x}	\bar{y}	\bar{x}	\bar{y}
$\alpha = 1.0, \kappa = 0.0, n = 1.0$	0.87999	0.42921	0.87988	0.42953	0.88055	0.42764
$\alpha = 1.0, \kappa = 0.2, n = 1.0$	0.81734	0.51390	0.81715	0.51429	0.81820	0.51204
$\alpha = 1.0, \kappa = -0.6, n = 1.0$	0.99785	0.04565	0.99784	0.04560	0.99785	0.04586
$\alpha = 0.2, \kappa = -0.6, n = 0.5$	0.95853	-0.24187	0.95847	-0.24212	0.95887	-0.24063

from the analytical solution up to $\alpha = 2.6$ (Fig. 5b). Hence, the procedure II is computationally more effective than procedure I. From now onwards, only procedure II will be referred as the Adomian decomposition method.

The solutions obtained from Adomian decomposition method have been compared numerically with the existing elliptic integral solutions and are also presented in Table 1. The accuracy up to two decimal places can be noted. The convergence of the Adomian decomposition method for the present problem is demonstrated in Table 2. Here, the coordinates of the end point

of the beam are computed for increasing number of terms in the Adomian polynomial. It proves that inclusion up to the 8th term in the Adomian polynomial is sufficient.

The Adomian decomposition method can be used to determine the deformed beam shape for combined end loading as well. Fig. 5c shows two sets of beam configurations due to combined end loading, one without and the other with an inflection point corresponding to Cases A and B, respectively.

The advantage of the Adomian decomposition method is that once the closed form expression is obtained, it can be used for

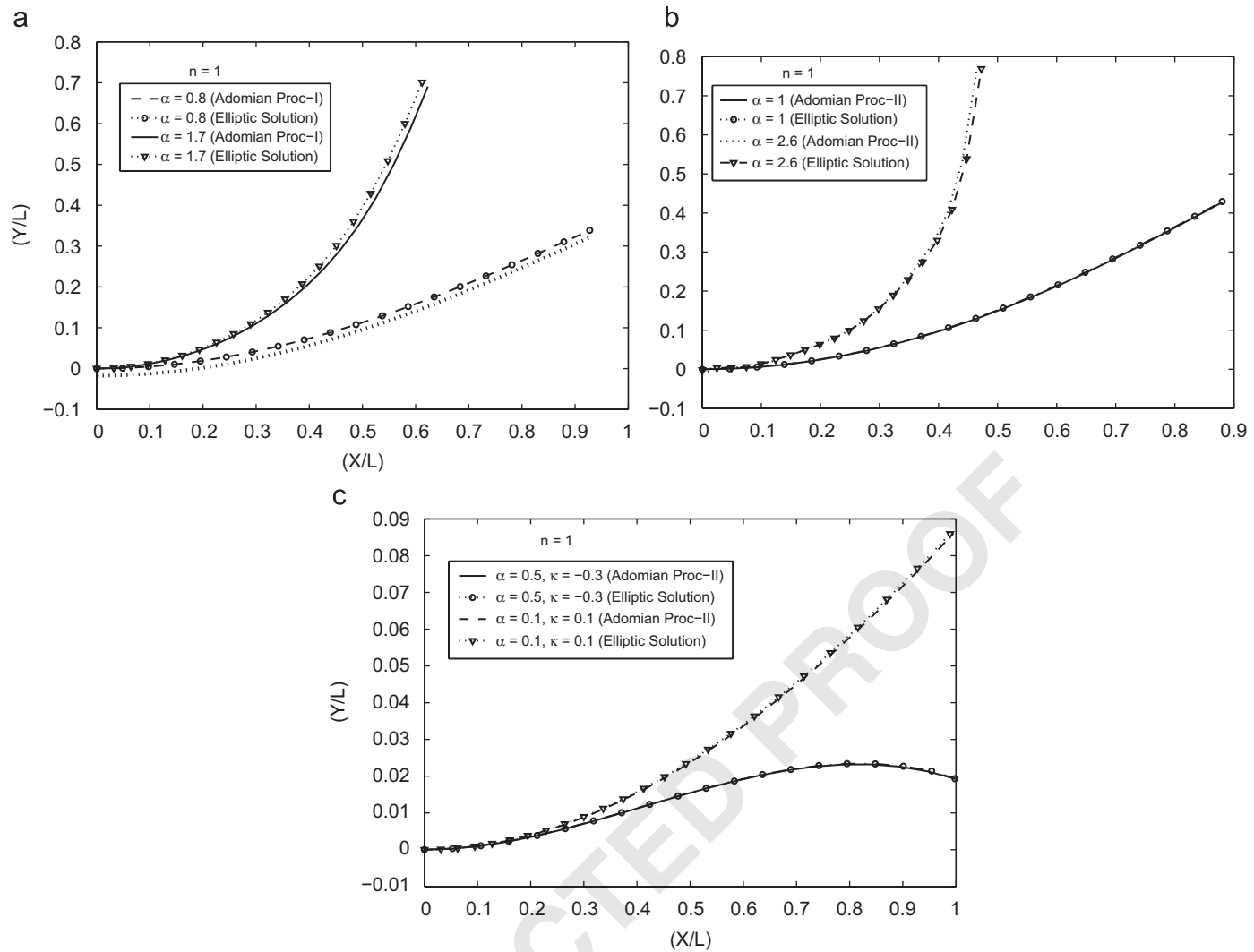


Fig. 5. (a) Beam configuration due to end forces; (b) beam configuration due to end forces; (c) beam configuration due to combined end loading.

Table 2
Proof of convergence of Adomian decomposition method

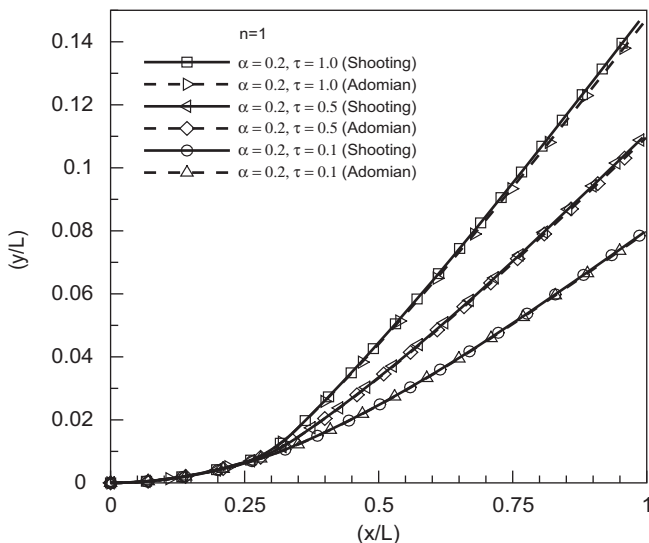
Number of terms in Adomian polynomial	At $\bar{s} = 1$ for $\alpha = 1.4, \kappa = 0.0, n = 1.0$	
	\bar{x}	\bar{y}
1	0.14866	0.78953
2	0.78308	0.55860
3	0.76760	0.57387
4	0.75247	0.58839
5	0.77050	0.57118
6	0.76326	0.57820
7	0.76471	0.57681
8	0.76454	0.57611
9	0.76461	0.57691

- 1 various values of loading parameters without recalling the program each time. However, with increasing load, more number
 3 of terms in the polynomial needs to be retained for the same level of accuracy. In this method, the unknown $c = \frac{d\theta}{ds}|_{s=0}$ is
 5 determined satisfying the second boundary condition given in Eq. (4). Satisfying the moment boundary condition specified

at the free end, higher order polynomials in ' c ' is obtained, hence multiple solutions are obvious. Depending on each and every real value of ' c ', a beam configuration can be obtained, for which the bending moment (curvature) at the fixed end can be calculated using Eq. (1). If the calculated value of the curvature at $s = 0$ match with the value of c , then the solution corresponding to that particular c is valid. Using this algorithm only one valid beam configuration has been obtained.

Figs. 6a and b show the deformed beam configuration obtained by using Adomian decomposition and non-linear shooting methods. In each case, actuating moments are assumed to be acting at $\frac{l_1}{L} = 0.25$ and $\frac{l_2}{L} = 0.35$, which implies that the length of the piezoelectric element, i.e., $(l_2 - l_1)$ is 10% of the length of the beam. Fig. 6a is obtained for a constant end force and various values of the positive actuating moments, while Fig. 6b is obtained for a constant negative actuating moment and various values of the end forces. It can be observed that each of the cases in Fig. 6b incorporates inflection point. For low values of the load parameters, both methods (non-linear shooting and Adomian decomposition method) yield almost the

a



b

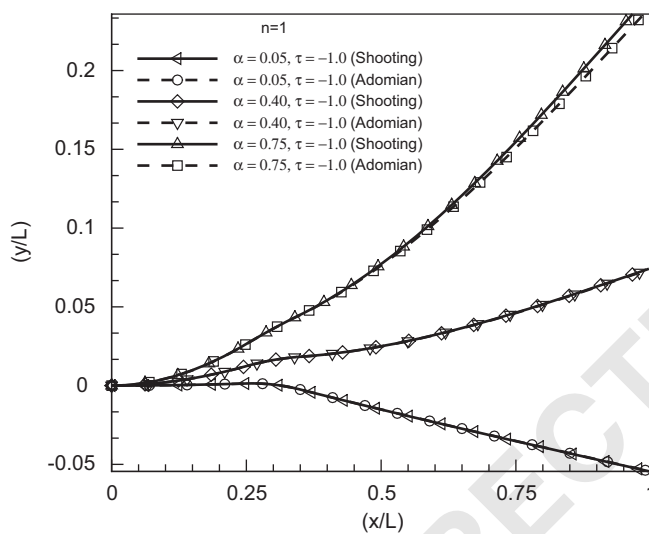


Fig. 6. (a) Beam configuration due to self-balanced moment and end forces; (b) beam configuration due to self-balanced moment and end forces.

1 same configuration. But with increasing load parameters, there
2 is a significant discrepancy between the two results, which can
3 be reduced by incorporating more number of terms in Adomian
4 polynomials.

5 All these results reveal that the non-linear shooting method is
6 very accurate and is independent of the value of loading param-
7 eters, but the program is to be recalled every time the loading
8 parameters are changed. Whereas for the Adomian decomposi-
9 tion method once the closed form expression is obtained, it can
10 be used for various values of loading parameters; but the maxi-
11 mum values of loading parameters are limited. Moreover, in the
12 Adomian method higher the number of discrete loadings, the
13 larger is the number of segments to be considered (as discussed
14 in Section 5.2), thus computational complexity increases. Over-
15 all, these two methods can be used to solve the large deflection
16 problem considering geometric non-linearity under any type of
17 static loading.

7. Conclusion

New variation of non-linear shooting and Adomian decom-
19 position methods have been developed, used and validated against
21 elliptic integral solution while determining large deflection of
23 a cantilever beam under arbitrary end loading conditions. The
25 possibility of multiple solutions with high end loading is dis-
27 cussed in the context of buckling of the beam-column. Further,
29 the same procedures can handle static, concentrated and/or dis-
31 cretely distributed loadings. These two methods can also be
33 used to analyze beams with arbitrary variation of geometry (for
35 which no closed form solution is possible) just by treating the
flexural rigidity as a function of the independent variable 's'. It
is observed that these methods are totally insensitive to the ex-
istence of any inflection point. These procedures are envisaged
to be useful for modeling the actuation of compliant mech-
anisms by discretely distributed smart actuators. In future, these
solution procedures will be extended to model multi-link com-
pliant mechanisms driven by smart actuators.

Acknowledgments

The authors would like to thank one of the anonymous re-
viewers for his constructive criticisms on an earlier version of
this paper. Thanks are also due to Prof. V. Raghavendra of
Mathematics Department and Dr. I. Sharma of Mechanical En-
gineering Department, IIT Kanpur, India.



Appendix A

The expression of $\theta(s)$ obtained using Adomian decomposi-
39 tion method (up to 6th order term) is $\theta(s) = \sum_{p=1}^{13} c_p * s^{(p-1)}$,
where

$$c1 := 0,$$

$$c2 := c,$$

$$c3 := \frac{1}{2}\kappa,$$

$$c4 := \frac{1}{6}\kappa nc,$$

$$c5 := \frac{1}{24}\kappa^2 n - \frac{1}{24}\kappa c^2,$$

$$c6 := \frac{1}{40}\kappa(-ck + \frac{1}{3}n^2\kappa c) - \frac{1}{120}\kappa nc^3,$$

$$c7 := \frac{1}{60}\kappa(-\frac{1}{4}\kappa^2 + \frac{1}{12}n^2\kappa^2) - \frac{11}{720}\kappa^2 c^2 n + \frac{1}{720}\kappa c^4,$$

$$c8 := \frac{1}{252}\kappa(-\frac{3}{2}ck^2 n + \frac{3}{20}nk(-ck + \frac{1}{3}n^2\kappa c)) \\ + \frac{1}{1008}\kappa(3c^3\kappa - \frac{11}{5}n^2c^3\kappa) + \frac{1}{5040}\kappa nc^5,$$

$$c9 := \frac{1}{336}\kappa(-\frac{1}{4}\kappa^3 n + \frac{1}{10}nk(-\frac{1}{4}\kappa^2 + \frac{1}{12}n^2\kappa^2)) \\ + \frac{1}{1344}\kappa(2c^2\kappa^2 - \frac{16}{5}\kappa^2 n^2 c^2 - \frac{3}{5}ck(-ck + \frac{1}{3}n^2\kappa c)) \\ + \frac{19}{13440}\kappa^2 c^4 n,$$

$$\begin{aligned} c10 := & \frac{1}{1728}\kappa(-\frac{7}{6}\kappa^3n^2c - \frac{2}{5}c\kappa(-\frac{1}{4}\kappa^2 + \frac{1}{12}n^2\kappa^2) \\ & - \frac{3}{10}\kappa^2(-c\kappa + \frac{1}{3}n^2\kappa c) + \frac{1}{2}c\kappa^3 \\ & + \frac{2}{21}n\kappa(-\frac{3}{2}c\kappa^2n + \frac{3}{20}n\kappa(-c\kappa + \frac{1}{3}n^2\kappa c))) \\ & + \frac{1}{8640}\kappa(\frac{5}{42}n\kappa(3c^3\kappa - \frac{11}{5}n^2c^3\kappa) + 14c^3\kappa^2n \\ & - \frac{3}{2}nc^2\kappa(-c\kappa + \frac{1}{3}n^2\kappa c) - \frac{5}{3}n^3c^3\kappa^2), \end{aligned}$$

$$\begin{aligned} c11 := & \frac{1}{2160}\kappa(-\frac{7}{48}\kappa^4n^2 - \frac{1}{5}\kappa^2(-\frac{1}{4}\kappa^2 + \frac{1}{12}n^2\kappa^2) + \frac{1}{16}\kappa^4 \\ & + \frac{1}{14}n\kappa(-\frac{1}{4}\kappa^3n + \frac{1}{10}n\kappa(-\frac{1}{4}\kappa^2 + \frac{1}{12}n^2\kappa^2))) \\ & + \frac{1}{10800}\kappa(-nc^2\kappa(-\frac{1}{4}\kappa^2 + \frac{1}{12}n^2\kappa^2) \\ & - 2\kappa^2nc(-c\kappa + \frac{1}{3}n^2\kappa c) + \frac{27}{4}\kappa^3c^2n - \frac{5}{3}n^3c^2\kappa^4 \\ & + \frac{5}{56}n\kappa(2c^2\kappa^2 - \frac{16}{5}\kappa^2n^2c^2 - \frac{3}{5}c\kappa(-c\kappa + \frac{1}{3}n^2\kappa c)) \\ & - \frac{10}{21}c\kappa(-\frac{3}{2}c\kappa^2n + \frac{3}{20}n\kappa(-c\kappa + \frac{1}{3}n^2\kappa c))), \end{aligned}$$

$$\begin{aligned} c12 := & \frac{1}{13200}\kappa(\frac{5}{72}n\kappa(-\frac{7}{6}\kappa^3n^2c - \frac{2}{5}c\kappa(-\frac{1}{4}\kappa^2 + \frac{1}{12}n^2\kappa^2) \\ & - \frac{3}{10}\kappa^2(-c\kappa + \frac{1}{3}n^2\kappa c) + \frac{1}{2}c\kappa^3 \\ & + \frac{2}{21}n\kappa(-\frac{3}{2}c\kappa^2n + \frac{3}{20}n\kappa(-c\kappa + \frac{1}{3}n^2\kappa c))) \\ & - \frac{5}{14}c\kappa(-\frac{1}{4}\kappa^3n + \frac{1}{10}n\kappa(-\frac{1}{4}\kappa^2 + \frac{1}{12}n^2\kappa^2)) \\ & - \frac{5}{21}\kappa^2(-\frac{3}{2}c\kappa^2n + \frac{3}{20}n\kappa(-c\kappa + \frac{1}{3}n^2\kappa c)) - \frac{25}{48}n^3c\kappa^4 \\ & - \frac{4}{3}\kappa^2nc(-\frac{1}{4}\kappa^2 + \frac{1}{12}n^2\kappa^2) \\ & - \frac{1}{2}\kappa^3n(-c\kappa + \frac{1}{3}n^2\kappa c) + \frac{65}{48}c\kappa^4n), \end{aligned}$$

$$\begin{aligned} c13 := & \frac{1}{15840}\kappa(-\frac{5}{28}\kappa^2(-\frac{1}{4}\kappa^3n + \frac{1}{10}n\kappa(-\frac{1}{4}\kappa^2 + \frac{1}{12}n^2\kappa^2)) \\ & - \frac{1}{3}\kappa^3n(-\frac{1}{4}\kappa^2 + \frac{1}{12}n^2\kappa^2) + \frac{13}{96}\kappa^5n - \frac{5}{96}\kappa^5n^3 \\ & + \frac{1}{18}n\kappa(-\frac{7}{48}\kappa^4n^2 - \frac{1}{5}\kappa^2(-\frac{1}{4}\kappa^2 + \frac{1}{12}n^2\kappa^2) + \frac{1}{16}\kappa^4 \\ & + \frac{1}{14}n\kappa(-\frac{1}{4}\kappa^3n + \frac{1}{10}n\kappa(-\frac{1}{4}\kappa^2 + \frac{1}{12}n^2\kappa^2))). \end{aligned}$$

5 Note: Obtained using Maple.

Appendix B

7 Consider the following BVP

$$\frac{d^2\theta}{ds^2} = (-\alpha \cos \theta - n\alpha \sin \theta) \quad (B.1)$$

9 with B.C.

$$\theta_{s=\alpha} = 0 \quad \text{and} \quad \frac{d\theta}{ds}_{s=b} = m.$$

11 Substituting $y(s) = \theta(s) - m(s-a)$ one obtains

$$\frac{d^2y}{ds^2} = (-\alpha \cos(y+m(s-a)) - n\alpha \sin(y+m(s-a))) \quad (B.2)$$

13 with $y_{s=a} = 0$ and $\frac{dy}{ds}_{s=b} = 0$.

This is a complete homogeneous BVP of second type as defined in Ref. [19] and its Green's function is given by

$$H(t, s) = \begin{cases} (s-a), & a \leq s \leq t, \\ (t-a), & t \leq s \leq b. \end{cases} \quad (B.3)$$

Let, $f(s, y(s)) = (-\alpha \cos(y+m(s-a)) - n\alpha \sin(y+m(s-a)))$. thus one gets

$$\frac{\partial f}{\partial y} = (\alpha \sin(y+m(s-a)) - n\alpha \cos(y+m(s-a))). \quad (B.4)$$

Eq. (B.4) can be written as

$$\begin{aligned} \frac{\partial f}{\partial y} &= (A \cos \beta \sin(y+m(s-a)) \\ &+ A \sin \beta \cos(y+m(s-a))) \\ &\equiv A \sin((y+m(s-a)) + \beta). \end{aligned} \quad (B.5)$$

Eq. (B.5) yields the Lipschitz's constant of the function $f(s, y(s))$ w.r.t. y as $|\frac{\partial f}{\partial y}|_{\max} = A$, which finally takes the form

$$A = \alpha\sqrt{1+n^2}. \quad (B.6)$$

Following the arguments in Ref. [19, p. 29, Eq. (3.19)] one obtains the mapping parameter λ as $\lambda = A \max_{a \leq t \leq b} [\frac{1}{w(t)} \int_a^b H(t, s)w(s) ds]$. If $\lambda \leq 1$, then the mapping is a contraction mapping and thus from the principle of contraction mapping the BVP possess unique solution. In order to obtain $w(t)$ the extreme case has been considered, i.e.,

$$A \left[\frac{1}{w_0}(t) \int_a^b H(t, s)w_0(s) ds \right] = 1. \quad (B.7)$$

This function $w_0(t)$ is positive in the interval (a, b) and vanishes at a and b . From the definition of Green's function one can say that Eq. (B.7) denotes the solution of the following BVP.

$$\text{D.E. } w_0''(t) + Aw_0(t) = 0,$$

$$\text{B.C. } w_0(a) = 0 \quad \text{and} \quad w_0'(b) = 0. \quad (B.8)$$

This problem has a non-trivial solution if

$$\sqrt{A}(b-a) = (2k+1)\frac{\pi}{2} \quad \text{where } k = 0, 1, 2, \dots. \quad (B.9)$$

For the minimum value of $k = 0$ one obtains $\sqrt{A}(b-a) = \frac{\pi}{2}$. Thus, in order to have $\lambda \leq 1$ one must have

$$\sqrt{A}(b-a) \leq \frac{\pi}{2} \equiv A(b-a)^2 \leq \frac{\pi^2}{4}. \quad (B.10)$$

Substituting (B.6) in (B.9) the final form of the condition to ensure uniqueness is obtained as

$$\alpha\sqrt{1+n^2} \leq \frac{\pi^2}{4(b-a)^2}. \quad (B.11)$$

For the current problem with $a = 0$ and $b = 1$ the final form becomes

$$\alpha\sqrt{1+n^2} \leq \frac{\pi^2}{4}. \quad (B.12)$$

1 References

- [1] K.E. Bisshop, D.C. Drucker, Large deflection cantilever beams, *Q. Appl. Math.* 3 (1945) 272–275.
- [2] L.L. Howell, A. Midha, Parametric deflection approximations for end-loaded large deflection beams in compliant mechanisms, *ASME J. Mech. Des.* 117 (1995) 156–165.
- [3] A. Saxena, S.N. Kramer, A simple and accurate method for determining large deflections in compliant mechanisms subjected to end forces and moments, *ASME J. Mech. Des.* 120 (1998) 392–400.
- [4] C. Kimball, L.-W. Tsai, Modeling of flexural beams subjected to arbitrary end loads, *ASME J. Mech. Des.* 124 (2002) 223–234.
- [5] A. Stanoyevitch, *Introduction to Numerical Ordinary and Partial Differential Equations Using Matlab*, Wiley, NJ, 2005.
- [6] G. Adomian, *Solving Frontier Problems of Physics: The Decomposition Method*, Kluwer, Boston, 1994.
- [7] E.F. Crawley, J. Luis, Use of piezoelectric actuators as elements of intelligent structures, *AIAA J.* 25 (1987) 1373–1385.
- [8] E.F. Crawley, Intelligent structures for aerospace: a technology overview and assessment, *AIAA J.* 32 (1994) 1689–1699.
- [9] B.T. Wang, C.A. Rogers, Modeling of finite length spatially-distributed induced strain actuators for laminate beams and plates, *J. Intell. Mater. Syst. Struct.* 2 (1991) 38–58.
- [10] P. Gaudenzi, R. Barboni, Static adjustment of beam deflections by means of induced strain actuators, *Smart Mater. Struct.* 8 (1999) 278–283.
- [11] A. Wazwaz, A reliable algorithm for solving boundary value problems for higher-order integro-differential equations, *Appl. Math. Comput.* 118 (2001) 327–342.
- [12] I. Hashim, Adomian decomposition method for solving boundary value problems for fourth-order integro-differential equations, *J. Comput. Appl. Math.* 193 (2006) 658–664.
- [13] V. Seng, K. Abbaoui, Y. Cherrault, Adomian's polynomials for non-linear operators, *Math. Comput. Modeling* 24 (1996) 59–65.
- [14] A. Wazwaz, A new method for calculating Adomian polynomials for non-linear operators, *Appl. Math. Comput.* 111 (2000) 33–51.
- [15] Y. Cherrault, Convergence of Adomian method, *Math. Comput. Modeling* 14 (1990) 83–86.
- [16] Y. Cherrault, G. Saccomandi, B. Some, New results for convergence of Adomian's method applied to integral equations, *Math. Comput. Modeling* 16 (1992) 85–93.
- [17] Y. Cherrault, G. Adomian, Decomposition method: a new proof of convergence, *Math. Comput. Modeling* 18 (1993) 103–106.
- [18] K. Abbaoui, Y. Cherrault, Convergence of Adomian method applied to non-linear equations, *Math. Comput. Modeling* 20 (1994) 69–73.
- [19] P.B. Bailey, L.F. Shampine, P.E. Waltman, *Non-linear Two Point Boundary Value Problems*, Academic Press, New York, London, 1968.